

# A large, switchable optical clearing skull window for cerebrovascular imaging

Chao Zhang<sup>1,2</sup>, Wei Feng<sup>1,2</sup>, Yanjie Zhao<sup>1,2</sup>, Tingting Yu<sup>1,2</sup>, Pengcheng Li<sup>1,2</sup>, Tonghui Xu<sup>1,2</sup>, Qingming Luo<sup>1,2</sup>, Dan Zhu<sup>1,2</sup>✉

1. Britton Chance Center for Biomedical Photonics, Wuhan National Laboratory for Optoelectronics-Huazhong University of Science and Technology, Wuhan, Hubei 430074, China
2. MoE Key Laboratory for Biomedical Photonics, Collaborative Innovation Center for Biomedical Engineering, School of Engineering Sciences, Huazhong University of Science and Technology, Wuhan, Hubei 430074, China

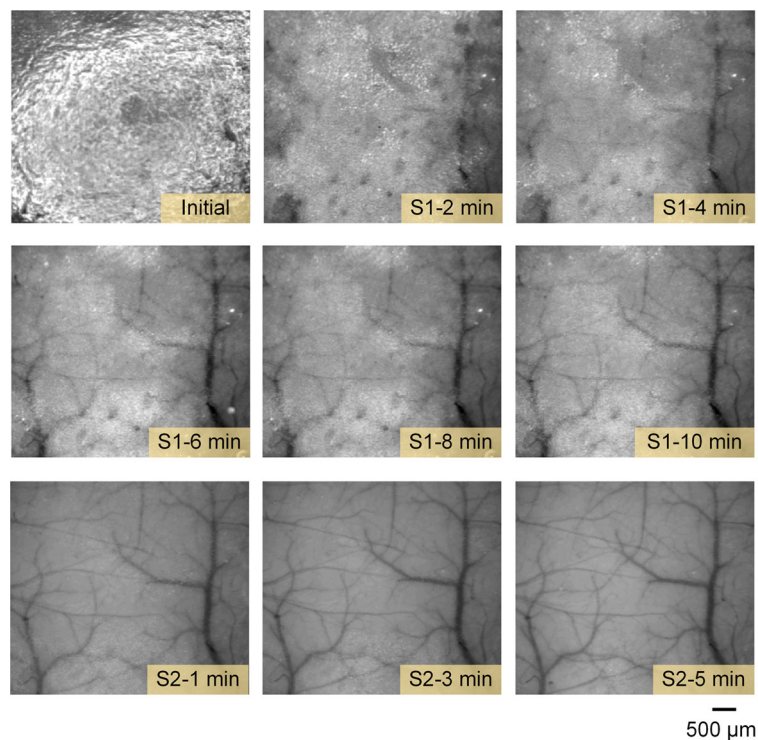


Figure S1. The white-light maps of cortical vessels observed through clearing skull at various time duration.

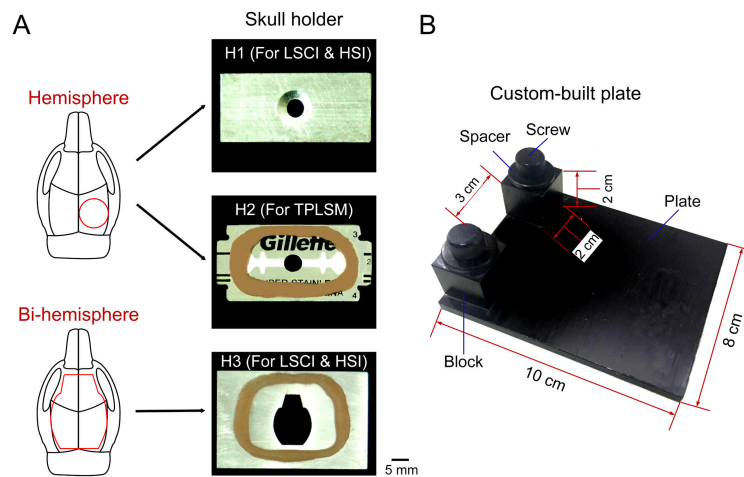
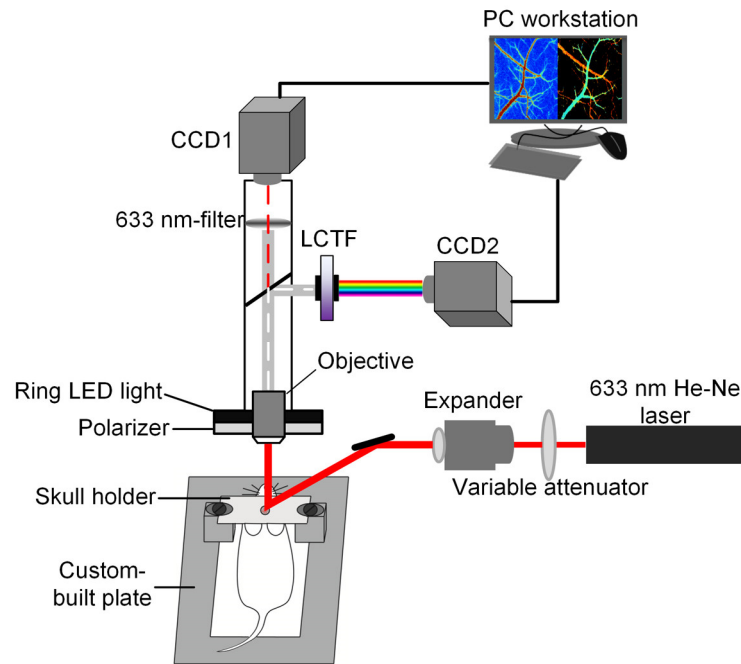
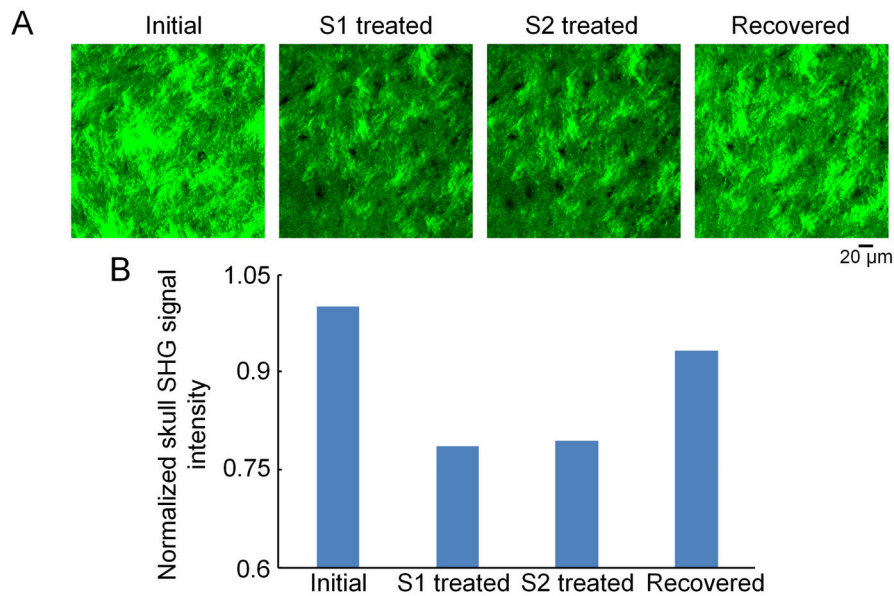


Figure S2. The photographs of metallic skull holders and custom-built plate. (A) H1: wide-field imaging of hemisphere; H2:

microscopic imaging of hemisphere; H3: wide-field imaging of bi-hemispheres. H1 and H3 are made of aluminum, and H2 is made by two razor blades glued together. Dental cement circles are glued on H2 and H3 for clearing agent storage. **(B)** The photograph of custom-built plate that consists of 1 plate, 2 blocks, 2 crews and 2 spacers.



**Figure S3. LSCI/HSI dual-modal system diagram.**



**Figure S4. SHG signals of the mouse skull in the same area. (A)** Skull SHG signals at initial, 10-min S1 treatment, 5-min S2 treatment and recovery conditions. Images (1024×1024 pixels, 0.2 μm/pixel) show maximum projections across 0-50μm, the z-step was 1 μm, the dwell time was 1 μs/pixel and the average power was 55 mW. (Excitation: 890 nm, detection: 445 ± 40 nm, objective: 16×W 0.8 NA, zoom factor: 3). **(B)** Bar graph of normalized average SHG signal intensities at initial, 10-min S1 treatment, 5-min S2 treatment and recovery conditions.

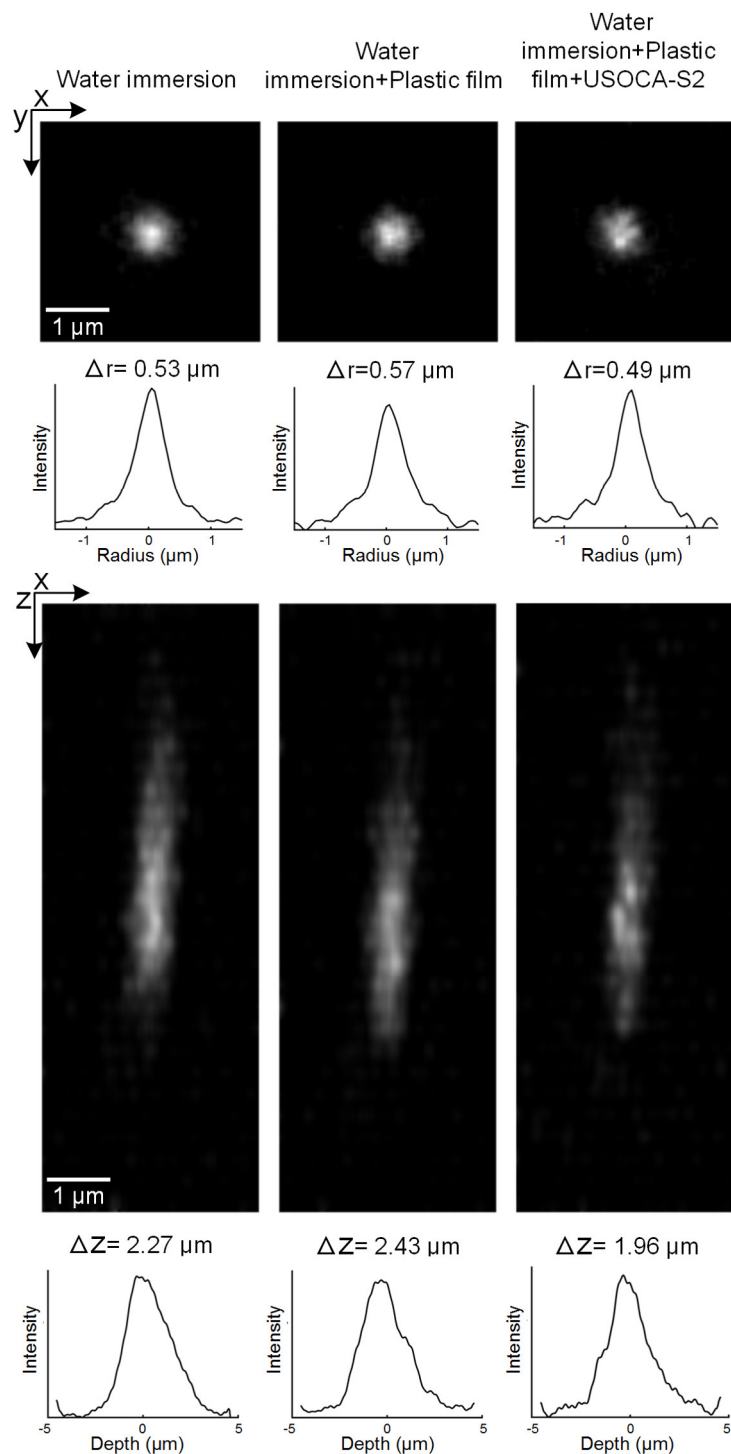


**Figure S5.** The first and second rows show the maximal projection (x-y) and radial depth profile of the integrated axial intensity along the radial axis, respectively. The third and fourth rows are the maximal projection (x-z) and axial depth profile of the integrated axial intensity along the z-axis, respectively. The first column is the fluorescent bead imaged by using only dipping objective. The second column is the fluorescent bead imaged under the plastic film with water dipping objective. The third column is a fluorescent bead imaged through clearing agent (USOCA-S2) and thin plastic film using water dipping objective. The  $\Delta r$  and  $\Delta z$  are the full widths that encompass half of the integrated intensity. Images in the first row (1024×1024 pixels, 0.05  $\mu\text{m}/\text{pixel}$ ) are maximum projections across 0-9.75 $\mu\text{m}$ , the z-step was 0.325  $\mu\text{m}$ , the dwell time was 1  $\mu\text{s}/\text{pixel}$  and the average power was 10 mW. (Excitation: 800 nm, detection: 525±25 nm, objective: 40× 0.8 NA, zoom factor: 6).

**Table S1. Changes in body weight and organ-to-body weight ratio of mice at initial state and the 28th day after treatment with USOCA.**

<b>Groups</b>	<b>Initial body weight(g)</b>	<b>Final Body weight(g)</b>	<b>Heart (%)</b>	<b>Liver (%)</b>	<b>Spleen (%)</b>	<b>Lung (%)</b>	<b>Kidney (%)</b>	<b>Brain (%)</b>
<b>Control</b>	22.34±1.02	24.48±1.33	0.57±0.01	5.41±0.13	0.61±0.01	0.58±0.03	1.87±0.03	1.84±0.02
<b>USOCA</b>	22.22±0.98	24.60±1.21	0.56±0.01	5.47±0.06	0.60±0.02	0.59±0.02	1.86±0.02	1.85±0.02